PHYSICAL REVIEW B **89**, 161116(R) (2014)

Magnetic-field-induced charge order in the filled skutterudite $SmRu_4P_{12}$: Evidence from resonant and nonresonant x-ray diffraction

Takeshi Matsumura,[1,2,*] Shinji Michimura,[3] Toshiya Inami,[4] Yuya Hayashi,[1] Kengo Fushiya,[5] Tatsuma D. Matsuda,[5] Ryuji Higashinaka,[5] Yuji Aoki,[5] and Hitoshi Sugawara[6]

[1]*Department of Quantum Matter, AdSM, Hiroshima University, Higashi-Hiroshima 739-8530, Japan*
[2]*Institute for Advanced Materials Research, Hiroshima University, Higashi-Hiroshima 739-8530, Japan*
[3]*Department of Physics, Faculty of Science, Saitama University, Saitama 338-8570, Japan*
[4]*Condensed Matter Science Division, Japan Atomic Energy Agency, Sayo, Hyogo 679-5148, Japan*
[5]*Department of Physics, Tokyo Metropolitan University, Hachioji, Tokyo 192-0397, Japan*
[6]*Department of Physics, Kobe University, Kobe 657-8501, Japan*

(Received 18 February 2014; revised manuscript received 2 April 2014; published 25 April 2014)

The antiferromagnetic ordered phase in $SmRu_4P_{12}$ below the metal-insulator transition at $T_{MI} = 16.5$ K with an unresolved transition at $T^* \sim 14$ K has been studied by resonant and nonresonant x-ray diffraction in magnetic fields. In the intermediate phase, a nonresonant Thomson scattering with $\boldsymbol{q} = (1,0,0)$ is induced by applying a magnetic field, which is presumably caused by atomic displacements reflecting the charge order in the p band, as predicted theoretically [R. Shiina, J. Phys. Soc. Jpn. **82**, 083713 (2013)]. Simultaneously, the antiferromagnetic moment of Sm is enhanced along the field direction, which is considered to reflect the staggered ordering of the $\Gamma_7 - \Gamma_8$ crystal-field states (scalar or hexadecapole order). The present results show that the orbital-dependent p-f hybridization in association with the nesting instability in the p band gives rise to the unconventional charge order similarly with $PrRu_4P_{12}$ and $PrFe_4P_{12}$.

DOI: 10.1103/PhysRevB.89.161116 PACS number(s): 71.27.+a, 71.30.+h, 75.25.Dk

Hybridization between localized and itinerant electrons gives rise to a variety of phenomena in strongly correlated electron systems, especially in f-electron systems where several crystal-field (CF) levels with different orbital symmetries are involved in the hybridization. In this sense, filled skutterudite compounds RT_4X_{12} (R = rare earth, T = transition metal, and X = P, As, and Sb) have attracted interest because of their wide variety of phenomena: hybridization-gap formation in both charge and spin channels in $CeOs_4Sb_{12}$ with an unresolved ordered phase [1,2], unconventional superconductivity in $PrOs_4Sb_{12}$ with an antiferroquadrupole ordered phase at high magnetic fields [3–6], metal-insulator transition in $PrRu_4P_{12}$ with staggered ordering of the CF states [7–12], and a similar ordering of totally symmetric parameter in $PrFe_4P_{12}$ [13–17]. The type of ordering mechanisms of the scalar parameter in $PrRu_4P_{12}$ and $PrFe_4P_{12}$ are strongly associated with the singlet-triplet CF states and their orbital-dependent hybridization with the p band [18–23]. Since the main conduction p band, which consists of the xyz-type molecular orbital of P_{12}, has a strong nesting instability with $\boldsymbol{q} = (1,0,0)$, the transport property is also associated with the ordering of the f states with $\boldsymbol{q} = (1,0,0)$ [24].

$SmRu_4P_{12}$ has also attracted interest because of its mysterious ordered phase below the metal-insulator transition at $T_{MI} = 16.5$ K [25–31]. It has been established that an antiferromagnetic (AFM) dipole order exists below T_{MI} by muon spin relaxation [32,33], nuclear magnetic and quadrupole resonance (NMR/NQR) [34–37], nuclear resonant forward scattering [38], and neutron diffraction [39]. What is intriguing is that a distinct anomaly reminiscent of another phase transition develops at $T^* \sim 14$ K in magnetic fields in the ordered phase [26–29]. To understand the intermediate phase ($T^* < T < T_{MI}$) consistently with the bulk properties, a possibility of a magnetic octupole as a primary order parameter has been proposed [40,41]. However, in spite of the intense experimental studies, the microscopic nature of the ordered phases in $SmRu_4P_{12}$ has remained unresolved.

Recently, Shiina proposed a theory to explain the ordered phases of $SmRu_4P_{12}$ based on the p-f hybridization Hamiltonian, which was used to explain the unconventional charge order (CO) in $PrRu_4P_{12}$ and $PrFe_4P_{12}$ [42], i.e., the charge-density-wave formation in the p band and the scalar or hexadecapole order in the f state. The crucial part of the Hamiltonian is effectively written as

$$\mathcal{H}_{pf} = J_s \sum_i \hat{\boldsymbol{\sigma}}_i \cdot \hat{\boldsymbol{s}}_i + J_c \sum_i \delta\hat{n}_i \cdot \hat{\phi}_i, \qquad (1)$$

where the first term represents the spin interaction between the f electron in the Γ_7 doublet ($\hat{\boldsymbol{s}}_i$) and the conduction electron in the p band ($\hat{\boldsymbol{\sigma}}_i$). This leads to the AFM order of the Sm spins in the Γ_7 state. It is noted that the p electron hybridizes only with the Γ_7 f state by symmetry. The second term represents the charge interaction, where $\delta\hat{n}_i$ represents the deviation of the number of conduction electrons from unity at the ith Sm site and $\hat{\phi}_i$ represents the occupancy of the Γ_7 ($\hat{\phi} = 1$) and Γ_8 ($\hat{\phi} = 0$) CF states. This leads to the CO of the p electrons with the staggered ordering of the $4f$ CF states.

An important consequence of this model is that the CO is induced by a magnetic field in the AFM phase in a narrow temperature range near T_N ($T^* < T < T_{MI} = T_N$), which well explains the phase diagram. A schematic illustration of the ordered state is shown in Fig. 1, which is based on Ref. [42] and the present experimental results. This unconventional CO

*tmatsu@hiroshima-u.ac.jp

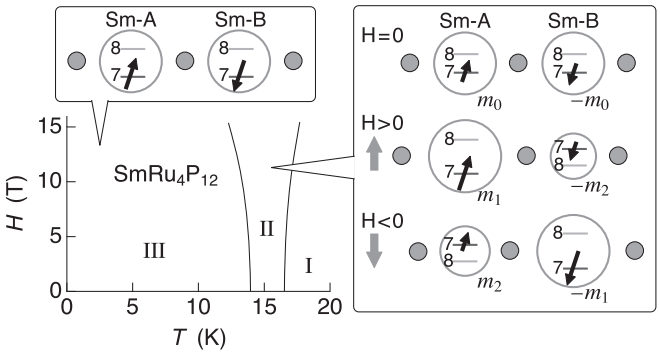

FIG. 1. The magnetic phase diagram of $SmRu_4P_{12}$ from Ref. [26] and schematic illustrations of the ordered states based on Ref. [42] with additional information of the field-induced atomic displacements and the field-reversal effect. Sm-A and Sm-B ions are at the corner and the center of the bcc lattice, respectively. The z components of the magnetic moments are represented by m_0, m_1, and m_2. The indices 7 and 8 represent the Γ_7 and Γ_8 CF states, respectively, of the $4f$ orbital. The circles at the Sm site represent the number of conduction electrons (charge) at the Sm site. The small gray circles schematically represent the surrounding atoms, whose displacement is associated with the CO.

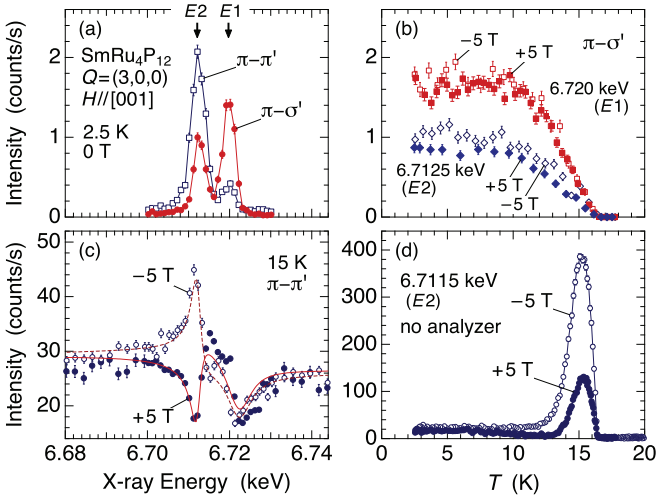

FIG. 2. (Color online) (a) X-ray energy dependencies of the intensity at zero field and 2.5 K for π-π' and π-σ'. The error bars, as in other figures, represent one standard deviation. (b) Temperature dependencies of the $E1$ and $E2$ resonance intensities for π-σ' in magnetic fields of ± 5 T. (c) X-ray energy dependencies of the intensity at ± 5 T and 15 K for π-π'. Solid and dashed curves are the fits. (d) Temperature dependencies of the intensity at the $E2$ resonance energy at ± 5 T without polarization analysis. The background intensity of 25 cps has been subtracted.

is in contrast to those in $PrRu_4P_{12}$ and $PrFe_4P_{12}$, which are realized at zero field as stable ordered phases. This contrast arises mainly from the difference in the CF level scheme, which leads to the difference in hybridization and the difference in J_s and J_c. Thus, although the basic mechanism of the unconventional CO is similar to $PrRu_4P_{12}$ and $PrFe_4P_{12}$, the resultant phenomenon in $SmRu_4P_{12}$ is much different.

In this Rapid Communication, we present strong evidence for the field-induced CO predicted in Ref. [42]. One is the field-induced Thomson (charge) scattering, which is presumably caused by atomic displacements reflecting the CO. The second is the enhancement of the AFM moment along the field direction in the CO state, which provides evidence for the underlying order of the CF states.

The single-crystal sample was grown by a tin-flux method. Resonant and nonresonant x-ray diffraction has been performed at BL22XU in SPring-8 using x-ray energies near the L_3 edge of Sm. The incident x ray is almost perfectly polarized in the scattering plane (π polarization). The polarization of the diffracted beam was analyzed using the 220 reflection of a Cu crystal, with which the scattering angle is 92.41° at 6.720 keV. The sample, with a mirror polished (100) surface with $\sim 1 \times 1$ mm^2 in size, was mounted in an 8 T superconducting cryomagnet. The magnetic field was applied along the [001] axis.

At the lowest temperature of 2.5 K in phase III, we detected resonant peaks at $\boldsymbol{Q} \equiv \boldsymbol{k} - \boldsymbol{k}' = (3,0,0)$, where the Bragg diffraction from the fundamental lattice is forbidden. The energy spectra at zero field for π-σ' and π-π' channels are shown in Fig. 2(a). Two resonant peaks are clearly observed at 6.7125 and 6.720 keV, which can be ascribed to the $E2$ ($2p_{3/2}$-$4f$) and $E1$ ($2p_{3/2}$-$5d$) resonances, respectively. With increasing temperature, these peaks disappear at 16.5 K. The polarization analysis shows that the resonant signal consists of both π-σ' and π-π' contributions.

The magnetic structure factor $F_{\mathrm{M},\varepsilon\varepsilon'}$ is proportional to $\boldsymbol{m} \cdot (\boldsymbol{\varepsilon}' \times \boldsymbol{\varepsilon})$ for $E1$ and $\boldsymbol{m} \cdot \{(\boldsymbol{k}' \cdot \boldsymbol{k})(\boldsymbol{\varepsilon}' \times \boldsymbol{\varepsilon}) + (\boldsymbol{\varepsilon}' \cdot \boldsymbol{\varepsilon})(\boldsymbol{k}' \times \boldsymbol{k}) + (\boldsymbol{k}' \cdot \boldsymbol{\varepsilon})(\boldsymbol{\varepsilon}' \times \boldsymbol{k}) + (\boldsymbol{\varepsilon}' \cdot \boldsymbol{k})(\boldsymbol{k}' \times \boldsymbol{\varepsilon})\}$ for $E2$ [43,44], where $\boldsymbol{m}$ represents the magnetic moment of the Sm ion and $\boldsymbol{\varepsilon}$ ($\boldsymbol{\varepsilon}'$) represents the incident (final) polarization vector. The xyz axes are taken so that $\hat{\boldsymbol{x}} \parallel \boldsymbol{Q} = \boldsymbol{k} - \boldsymbol{k}'$, $\hat{\boldsymbol{y}} \parallel \boldsymbol{k} + \boldsymbol{k}'$, and $\hat{\boldsymbol{z}} \parallel \boldsymbol{k} \times \boldsymbol{k}' \parallel \boldsymbol{H}$. For $\boldsymbol{Q} = (3,0,0)$ and for both $E1$ and $E2$, $F_{\mathrm{M},\pi\sigma'}$ arises from m_x and m_y, and $F_{\mathrm{M},\pi\pi'}$ arises from m_z. The direction of $\boldsymbol{m}$ is considered to be along [111] from NMR, NQR, and a mean-field analysis [35,36,41]. If we assume $\boldsymbol{m} \parallel [111]$ and the equal populations of the $\langle 111\rangle$, $\langle \bar{1}11\rangle$, $\langle 1\bar{1}1\rangle$, and $\langle \bar{1}\bar{1}1\rangle$ domains, we have the calculated intensity ratios $I_{\pi\sigma'}/I_{\pi\pi'} = 2.5$ for $E1$ and 0.3 for $E2$, which are roughly consistent with the observation in Fig. 2(a). Therefore, by considering a possibility of unequal domain populations, which slightly modifies the intensity ratio, the origin of the resonant signals can be attributed to the AFM order with $\boldsymbol{m} \parallel [111]$. The AFM ordering is robust to the application of magnetic fields. As can be seen in Figs. 2(a) and 2(b), the resonant intensities for π-σ' are little affected by the field of 5 T.

The most remarkable finding in the present study is the appearance of the nonresonant charge scattering, which is induced by a magnetic field in phase II. As shown in Fig. 2(c), the energy spectrum at 15 K and 5 T for π-π' consists of a large contribution from nonresonant scattering and anomalies at $E2$ and $E1$ resonance energies. By contrast, the energy spectrum for π-σ' is identical to that at 2.5 K shown in Fig. 2(a) with reduced intensity as read from Fig. 2(b). Another important characteristic in Fig. 2(c) is the significant field-reversal asymmetry at 6.7115 keV ($E2$), which results from the interference between nonresonant charge scattering

and the $E2$ resonance of magnetic origin. The field-reversal asymmetry also exists at the $E1$ resonance. However, we do not deal with the $E1$ signal because it is disturbed by the dip anomaly around 6.720 keV due to the absorption. We concentrate on the clear interference effect at the $E2$ energy.

Figure 2(d) shows the temperature dependencies of the intensity at ±5 T at 6.7115 keV ($E2$), where the strongest interference effect is observed. The measurement was performed without an analyzer to improve the statistics. The large intensity in phase II above ∼13 K can fairly be regarded as arising from the π-π' scattering [see the different count rates in Figs. 2(b) and 2(c)]. The finite intensity at the lowest temperature consists of both π-π' and π-σ', as shown in Fig. 2(a).

Let us analyze the charge-magnetic interference in the π-π' channel. The energy-dependent structure factor for the $\boldsymbol{\varepsilon}$-$\boldsymbol{\varepsilon'}$ scattering process can be written as

$$F_{\varepsilon\varepsilon'}(\omega) = F_{\mathrm{C},\varepsilon\varepsilon'} + \{\alpha'_{E2}(\omega) + i\alpha''_{E2}(\omega)\} i F_{\mathrm{M},\varepsilon\varepsilon'}, \qquad (2)$$

where F_{C} and F_{M} represent the charge and magnetic structure factors at $\boldsymbol{Q} = (3,0,0)$, respectively. They interfere with each other in the π-π' channel. Note that $F_{\mathrm{C},\pi\sigma'} = 0$ and no interference occurs in the π-σ' channel. $\alpha_{E2}(\omega) = \alpha'_{E2}(\omega) + i\alpha''_{E2}(\omega)$ is the spectral function of the $E2$ resonance for the magnetic dipole order [44].

The field-reversal asymmetry shown in Fig. 2(c) is caused by the change in sign of either $F_{\mathrm{C},\pi\pi'}$ or $F_{\mathrm{M},\pi\pi'}$. If we assume $F_{\mathrm{C},\pi\pi'}$ is due to some atomic displacement induced by the CO, as schematically illustrated in Fig. 1, then $F_{\mathrm{C},\pi\pi'}$ changes sign when the field is reversed. On the other hand, $F_{\mathrm{M},\pi\pi'}$ does not change sign since $F_{\mathrm{M},\pi\pi'} \propto m_1 - (-m_2)$ for $H > 0$ and $F_{\mathrm{M},\pi\pi'} \propto m_2 - (-m_1)$ for $H < 0$ in Fig. 1. The solid and dashed curves in Fig. 2(c) are the fits using a single-oscillator spectral function, $\alpha_{E2}(\omega) = \Gamma e^{i\phi}/(\hbar\omega - \Delta + i\Gamma)$, where Δ, Γ, and ϕ are the energy, width, and phase factor of the $E2$ resonance, respectively. With $\Delta = 6.7123$, $\Gamma = 0.0014$, $\phi = -0.77\pi$, $F_{\mathrm{C},\pi\pi'} = \pm 5.6$, and $F_{\mathrm{M},\pi\pi'} = 1.5$, the spectrum for ±5 T can be well reproduced. The dip anomaly at 6.72 keV is the absorption effect.

Therefore, by changing the sign of $F_{\mathrm{C},\pi\pi'}$ in Eq. (2) for the reversed field, we obtain the average and difference intensities, $\bar{I} \equiv (I_+ + I_-)/2$ and $\Delta I \equiv (I_+ - I_-)/2$, respectively, for the ε-ε' channel as follows:

$$\bar{I}_{\varepsilon\varepsilon'} = |F_{\mathrm{C},\varepsilon\varepsilon'}|^2 + |\alpha_{E2} F_{\mathrm{M},\varepsilon\varepsilon'}|^2, \qquad (3)$$

$$\Delta I_{\varepsilon\varepsilon'} = -2\alpha''_{E2} F_{\mathrm{C},\varepsilon\varepsilon'} F_{\mathrm{M},\varepsilon\varepsilon'}. \qquad (4)$$

The T dependencies of $\bar{I}$ and ΔI at $\hbar\omega = 6.7115$ keV ($E2$) are shown in Fig. 3(a). Above ∼13 K, $\bar{I}$ is dominated by the nonresonant intensity from $|F_{\mathrm{C},\pi\pi'}|^2$; the magnetic contribution from $|F_{\mathrm{M},\pi\pi'}|^2$ and $|F_{\mathrm{M},\pi\sigma'}|^2$ is hard to identify. At low temperatures below ∼10 K, where $|F_{\mathrm{C},\pi\pi'}|^2$ completely vanishes, $\bar{I}$ consists of $|F_{\mathrm{M},\pi\pi'}|^2$ and $|F_{\mathrm{M},\pi\sigma'}|^2$, whose respective contributions are given in Fig. 2(a).

The T dependencies of $F_{\mathrm{C},\pi\pi'}$ and $F_{\mathrm{M},\pi\sigma'}$ can be directly obtained by taking the square root of the nonresonant intensity in Fig. 3(a) and the $E2$ intensity in Fig. 2(b), respectively. We note that $F_{\mathrm{C},\pi\pi'}$(6.7115 keV) can be substituted with $F_{\mathrm{C},\pi\pi'}$(6.680 keV), since we observe in Fig. 2(c) that $\bar{I}_{\pi\pi'}(\omega)$

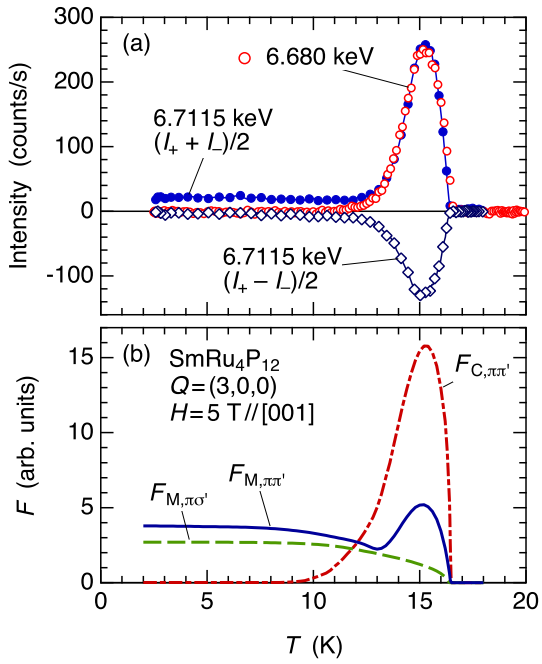

FIG. 3. (Color online) (a) Temperature dependencies of the average and difference intensities for ±5 T at the $E2$ resonance energy, which were deduced from the data in Fig. 2(d). The nonresonant intensity at +5 T measured at 6.680 keV is also shown. The background intensity has been subtracted. (b) Temperature dependencies of the charge and magnetic structure factors to explain the results in (a).

around the $E2$ energy is almost constant and equal to $\bar{I}_{\pi\pi'}$(6.680 keV). To deduce the T dependence of $F_{\mathrm{M},\pi\pi'}$, we need to use $\bar{I}$ and Eq. (3) in the low-T region where $F_{\mathrm{C},\pi\pi'}$ vanishes, whereas in the region where $\bar{I}$ is dominated by $|F_{\mathrm{C},\pi\pi'}|^2$, we need to use ΔI and Eq. (4). The threshold temperature is in a range of 12 ± 1 K. The resultant T dependencies of $F_{\mathrm{C},\pi\pi'}$, $F_{\mathrm{M},\pi\sigma'}$, and $F_{\mathrm{M},\pi\pi'}$ thus obtained, which well reproduce the results of $\bar{I}$ and ΔI in Fig. 3(a), are shown in Fig. 3(b).

Remarkably, $F_{\mathrm{M},\pi\pi'}$ exhibits an anomalous enhancement in phase II simultaneously with $F_{\mathrm{C},\pi\pi'}$. By contrast, $F_{\mathrm{M},\pi\sigma'}$ smoothly decreases with increasing temperature as in normal AFM orderings. It is noted again that $F_{\mathrm{M},\pi\sigma'}$ and $F_{\mathrm{M},\pi\pi'}$ reflect the xy components ($\perp H$) and the z component ($\parallel H$), respectively, of the AFM moments. The enhancement of $F_{\mathrm{M},\pi\pi'}$ by the field, therefore, is difficult to understand in the framework of normal AFM orderings, where a spin flip is expected to take place. It can be understood by considering the staggered ordering of the CF states as illustrated in Fig. 1, where $2m_0 < m_1 + m_2$ is satisfied.

Figure 4 shows the field dependence of the charge scattering. It is weakly induced at low fields and rapidly enhanced at high fields. This enhancement is consistent with that of the anomaly in the thermodynamic properties, which is also enhanced by the field around T^* [28,29,40]. The field dependence of $F_{\mathrm{C},\pi\pi'}$ at 15 K is shown in Fig. 4(b). At low fields below 2 T, $F_{\mathrm{C},\pi\pi'}$ increases linearly with H, whereas it exhibits a nonlinear increase above 2 T. This is also consistent

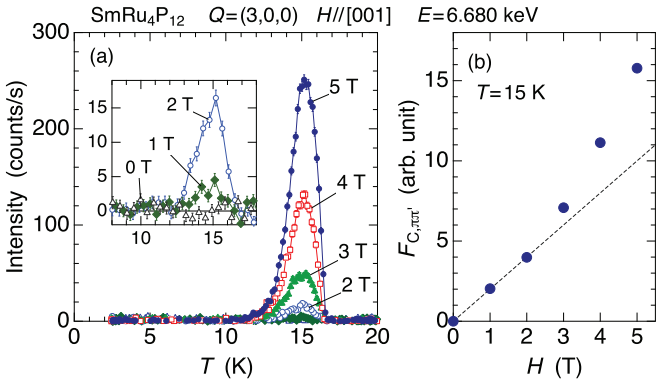

FIG. 4. (Color online) (a) Temperature dependencies of the nonresonant intensity at 6.680 keV in magnetic fields. The background intensity has been subtracted. (b) Magnetic field dependence of the charge structure factor at 15 K.

with the calculation by Shiina [45]. It should be noted, however, that the charge scattering vanishes at zero field, as shown in the inset of Fig. 4(a), whereas the anomaly around T^* weakly remains at zero field in the thermodynamic properties. From the T-dependence curves of Fig. 4(a), it seems that the II-III phase boundary corresponds to the inflection point and can be extrapolated to zero field, as shown in the phase diagram of Fig. 1. There is a possibility that the charge scattering was too weak to be detected at zero field.

The field-induced charge scattering is presumably caused by some atomic displacement as in $PrRu_4P_{12}$ and $PrFe_4P_{12}$ [8,9,14]. Although it has not been identified yet, the signal may naturally be interpreted as reflecting the field-induced CO, which is represented by ϕ_Q in Ref. [42], i.e., the ordering of $\hat{\phi}$ in Eq. (1) with $\boldsymbol{q} = (1,0,0)$. The simultaneous enhancement of $F_{M,\pi\pi'}$ observed in Fig. 3(b) can be directly compared with s_Q in Ref. [42]. It is noted that the enhancement of $F_{M,\pi\pi'}$ in phase II is much more pronounced than the calculation. This may be because the actual CF ground state is the Γ_8 quartet as deduced from the magnetic entropy [28], whereas no CF splitting is assumed in the theory. As discussed in Ref. [42], in the case of the Γ_8 ground state, the enhancement of s_Q should be more pronounced. This is consistent with the present result.

Another point to be noted is on the II-III phase boundary. Although the observed transition across T^* is smooth and continuous, the theory predicts that the transition can be of first order when the Γ_8 is the ground state. One reason for the continuous transition is that the field direction in the present study is [001], and not the [111] as assumed in the theory. This issue of the order of the transition is an interesting subject to be studied in more detail at higher fields and for other field directions.

In conclusion, we have detected strong evidence for the magnetic-field-induced CO in the intermediate phase ($T^* < T < T_{MI} = T_N$) of $SmRu_4P_{12}$, which has been the subject of much debate. In this phase, a nonresonant charge scattering is induced by the field at the forbidden Bragg spot $\boldsymbol{q} = (1,0,0)$, which coincides with the nesting vector of the filled skutterudite compounds. The charge scattering is presumably caused by atomic displacements reflecting the CO (charge-density-wave formation) in the p band, which has been theoretically predicted. In addition, by utilizing the charge-magnetic interference effect in resonant scattering, we have shown that the AFM component along the field direction is simultaneously enhanced. This provides strong evidence for the staggered ordering of the $\Gamma_7 - \Gamma_8$ CF states, which is directly associated with the CO. In the low-temperature phase ($T < T^*$), the field-induced signals disappear and the normal AFM order recovers. These behaviors in magnetic fields can be consistently understood as consequences of the competing nature of magnetic and charge interactions, where the CF- (orbital)-dependent p-f hybridization and the nesting instability in the p band play fundamental roles. Although the basic mechanism is similar to those of Pr-based skutterudites, the more competing nature of the relevant order parameters makes the phenomenon more drastic in $SmRu_4P_{12}$.

The authors thank R. Shiina for valuable discussions. This work was supported by Grants-in-Aid for Scientific Research (No. 21204456, No. 21102515, and No. 2430087) from JSPS and MEXT, and by a Basic Science Research Grant from the Sumitomo Foundation. The synchrotron radiation experiment was performed under Proposal No. 2013B3711 at BL22XU of SPring-8.

[1] D. T. Adroja, J.-G. Park, E. A. Goremychkin, K. A. McEwen, N. Takeda, B. D. Rainford, K. S. Knight, J. W. Taylor, J. Park, H. C. Walker, R. Osborn, and P. S. Riseborough, Phys. Rev. B **75**, 014418 (2007).

[2] M. Matsunami, R. Eguchi, T. Kiss, K. Horiba, A. Chainani, M. Taguchi, K. Yamamoto, T. Togashi, S. Watanabe, X.-Y. Wang, C.-T. Chen, Y. Senba, H. Ohashi, H. Sugawara, H. Sato, H. Harima, and S. Shin, Phys. Rev. Lett. **102**, 036403 (2009).

[3] E. D. Bauer, N. A. Frederick, P.-C. Ho, V. S. Zapf, and M. B. Maple, Phys. Rev. B **65**, 100506(R) (2002).

[4] G. Seyfarth, J. P. Brison, M.-A. Measson, J. Flouquet, K. Izawa, Y. Matsuda, H. Sugawara, and H. Sato, Phys. Rev. Lett. **95**, 107004 (2005).

[5] E. D. Bauer, P.-C. Ho, M. B. Maple, T. Schauerte, D. L. Cox, and F. B. Anders, Phys. Rev. B **73**, 094511 (2006).

[6] M. B. Maple, Z. Henkie, W. M. Yuhasz, P.-C. Ho, T. Yanagisawa, T. A. Sayles, N. P. Butch, J. R. Jeffries, and A. Pietraszko, J. Magn. Magn. Mater. **310**, 182 (2007).

[7] C. Sekine, T. Uchiumi, I. Shirotani, and T. Yagi, Phys. Rev. Lett. **79**, 3218 (1997).

[8] C. H. Lee, H. Matsuhata, H. Yamaguchi, C. Sekine, K. Kihou, T. Suzuki, T. Noro, and I. Shirotani, Phys. Rev. B **70**, 153105 (2004).

[9] D. Cao, R. H. Heffner, F. Bridges, I.-K. Jeong, E. D. Bauer, W. M. Yuhasz, and M. B. Maple, Phys. Rev. Lett. **94**, 036403 (2005).

[10] K. Iwasa, L. Hao, K. Kuwahara, M. Kohgi, S. R. Saha, H. Sugawara, Y. Aoki, H. Sato, T. Tayama, and T. Sakakibara, Phys. Rev. B **72**, 024414 (2005).
[11] K. Iwasa, L. Hao, T. Hasegawa, T. Takagi, K. Horiuchi, Y. Mori, Y. Murakami, K. Kuwahara, M. Kohgi, H. Sugawara, S. R. Saha, Y. Aoki, and H. Sato, J. Phys. Soc. Jpn. **74**, 1930 (2005).
[12] Y. Aoki, T. Namiki, S. R. Saha, T. Tayama, T. Sakakibara, R. Shiina, H. Shiba, H. Sugawara, and H. Sato, J. Phys. Soc. Jpn. **80**, 054704 (2011).
[13] H. Sato, Y. Abe, H. Okada, T. D. Matsuda, K. Abe, H. Sugawara, and Y. Aoki, Phys. Rev. B **62**, 15125 (2000).
[14] K. Iwasa, Y. Watanabe, K. Kuwahara, M. Kohgi, H. Sugawara, T. D. Matsuda, Y. Aoki, and H. Sato, Physica B **312–313**, 834 (2002).
[15] J. Kikuchi, M. Takigawa, H. Sugawara, and H. Sato, J. Phys. Soc. Jpn. **76**, 043705 (2007).
[16] K. Iwasa, L. Hao, Y. Murakami, M. Kohgi, K. Kuwahara, H. Sugawara, T. D. Matsuda, Y. Aoki, H. Sato, J.-M. Mignot, and A. Gukasov, J. Phys. Soc. Jpn. Suppl. A **77**, 67 (2008).
[17] K. Iwasa, L. Hao, M. Kohgi, K. Kuwahara, J.-M. Mignot, H. Sugawara, Y. Aoki, T. D. Matsuda, and H. Sato, J. Phys. Soc. Jpn. **81**, 094711 (2012).
[18] T. Takimoto, J. Phys. Soc. Jpn. **75**, 034714 (2006).
[19] R. Shiina, J. Phys. Soc. Jpn. **79**, 044704 (2010).
[20] R. Shiina, J. Phys. Soc. Jpn. **81**, 024706 (2012).
[21] R. Shiina, J. Phys. Soc. Jpn. **81**, 105001 (2012).
[22] A. Kiss and Y. Kuramoto, J. Phys. Soc. Jpn. **75**, 103704 (2006).
[23] S. Hoshino, J. Otsuki, and Y. Kuramoto, J. Phys. Soc. Jpn. **80**, 033703 (2011).
[24] H. Harima, J. Phys. Soc. Jpn. Suppl. A **77**, 114 (2008).
[25] C. Sekine, T. Uchiumi, I. Shirotani, and T. Yagi, in *Science and Technology of High Pressure*, edited by M. H. Manghnani, W. J. Nellis, and M. F. Nicol (Universities Press, Hyderabad, 2000), p. 826.
[26] K. Matsuhira, Y. Hinatsu, C. Sekine, T. Togashi, H. Maki, I. Shirotani, H. Kitazawa, T. Takamasu, and G. Kido, J. Phys. Soc. Jpn. Suppl. **71**, 237 (2002).
[27] C. Sekine, I. Shirotani, K. Matsuhira, P. Haen, S. De Brion, G. Chouteau, H. Suzuki, and H. Kitazawa, Acta Phys. Pol. B **34**, 983 (2003).
[28] K. Matsuhira, Y. Doi, M. Wakeshima, Y. Hinatsu, H. Amitsuka, Y. Shimaya, R. Giri, C. Sekine, and I. Shirotani, J. Phys. Soc. Jpn. **74**, 1030 (2005).
[29] C. Sekine, Y. Shimaya, I. Shirotani, and P. Haen, J. Phys. Soc. Jpn. **74**, 3395 (2005).
[30] M. Matsunami, L. Chen, M. Takimoto, H. Okamura, T. Nanba, C. Sekine, and I. Shirotani, Phys. Rev. B **72**, 073105 (2005).
[31] D. Kikuchi, K. Tanaka, H. Aoki, K. Kuwahara, Y. Aoki, H. Sugawara, and H. Sato, J. Magn. Magn. Mater. **310**, e225 (2007).
[32] K. Hachitani, H. Fukazawa, Y. Kohori, I. Watanabe, C. Sekine, and I. Shirotani, Phys. Rev. B **73**, 052408 (2006).
[33] T. U. Ito, W. Higemoto, K. Ohishi, T. Fujimoto, R. H. Heffner, N. Nishida, K. Satoh, H. Sugawara, Y. Aoki, D. Kikuchi, and H. Sato, J. Phys. Soc. Jpn. **76**, 053707 (2007).
[34] K. Hachitani, H. Amanuma, H. Fukazawa, Y. Kohori, K. Koyama, K. Kumagai, C. Sekine, and I. Shirotani, J. Phys. Soc. Jpn. **75**, 124712 (2006).
[35] S. Masaki, T. Mito, N. Oki, S. Wada, and N. Takeda, J. Phys. Soc. Jpn. **75**, 053708 (2006).
[36] S. Masaki, T. Mito, M. Takemura, S. Wada, H. Harima, D. Kikuchi, H. Sato, H. Sugawara, N. Takeda, and G. Zheng, J. Phys. Soc. Jpn. **76**, 043714 (2007).
[37] S. Masaki, T. Mito, S. Wada, H. Sugawara, D. Kikuchi, H. Sato, M. Takigawa, N. Takeda, and G.-q. Zheng, J. Phys. Soc. Jpn. Suppl. A **77**, 206 (2008).
[38] S. Tsutsui, Y. Kobayashi, T. Okada, H. Haba, H. Onodera, Y. Yoda, M. Mizumaki, H. Tanida, T. Uruga, C. Sekine, I. Shirotani, D. Kikuchi, H. Sugawara, and H. Sato, J. Phys. Soc. Jpn. **75**, 093703 (2006).
[39] C.-H. Lee, S. Tsutsui, K. Kihou, H. Sugawara, and H. Yoshizawa, J. Phys. Soc. Jpn. **81**, 063702 (2012).
[40] M. Yoshizawa, Y. Nakanishi, M. Oikawa, C. Sekine, I. Shirotani, S. R. Saha, H. Sugawara, and H. Sato, J. Phys. Soc. Jpn. **74**, 2141 (2005).
[41] Y. Aoki, S. Sanada, D. Kikuchi, H. Sugawara, and H. Sato, J. Phys. Soc. Jpn. **76**, 113703 (2007).
[42] R. Shiina, J. Phys. Soc. Jpn. **82**, 083713 (2013).
[43] J. P. Hannon, G. T. Trammell, M. Blume, and D. Gibbs, Phys. Rev. Lett. **61**, 1245 (1988).
[44] T. Nagao and J. I. Igarashi, Phys. Rev. B **74**, 104404 (2006).
[45] R. Shiina, JPS Conf. Proc. (to be published).